Predicting the filling of ventilated cavities behind spillway aerators

Prediction du remplissage des cavités ventilés derrière des aérateurs d'évacuateurs de crûes

H. CHANSON, MIAHR
Senior Lecturer in Fluid Mechanics, Hydraulics and Environmental Engineering, Department of Civil Engineering, The University of Queensland, Brisbane QLD 4072, Australia

SUMMARY
Cavitation damage to spillway surfaces may be prevented with the use of aeration devices. These serve to introduce air into the layers close to the channel bottom in order to reduce cavitation erosion. Under some circumstances, the aerator can be drowned out, will cease to protect the spillway surface, and act potentially as a cavitation generator. This article analyses the conditions of filling. Then experimental data for ten aerator geometries are reviewed. Depending upon the aerator geometry, the cavity filling occurs when the Froude number is less than a critical value or when the ratio of the flow depth over the total offset is larger than a characteristic value.

RÉSUMÉ
Les aérateurs de fond sont installés sur les évacuateurs de crûes pour empêcher l'érosion par cavitation. Ils servent à introduire de l'air dans les filets d'eau proches de la surface du coursier, afin d'empêcher les dommages par cavitation. Dans certaines conditions, un aérateur peut être noyé, auquel cas il cesse de protéger le coursier, et peut agir comme un générateur de cavitation. Cet article décrit les conditions de remplissage (noyade) des aérateurs. Puis plusieurs résultats expérimentaux sont présentés. En fonction de la géométrie des aérateurs, le remplissage est possible pour des nombres de Froude inférieurs à une valeur critique, ou pour des profondeurs adimensionnelles supérieures à une valeur limite.

1 Introduction

At large head chutes and bottom outlets, the risks of cavitation damage on chute spillways can be significant. For velocities greater than 35 m/s, severe tolerances of surface finish are required to avoid cavitation (e.g. FALVEY 1982). The cost of cavitation resistant materials to protect surfaces is prohibitive. For these reasons, the spillway surface is protected from cavitation erosion by introducing air next to the spillway surface. Air is introduced artificially by aeration devices located on the spillway floor and sometimes on the sidewalls.
A small deflection in a spillway structure (e.g. ramp, offset) deflects the high velocity flow away from the spillway surface (Fig. 1). In the cavity formed below the nappe, a local pressure depression (i.e. subpressure) ΔP is produced by which air is entrained into the flow.

Aerator filling

When the local pressure within the ventilated cavity drops severely, the cavity downstream of the deflector may disappear and be filled or drowned. This is called the aerator filling: the process is

Revision received December 30, 1994. Open for discussion till December 31, 1995.

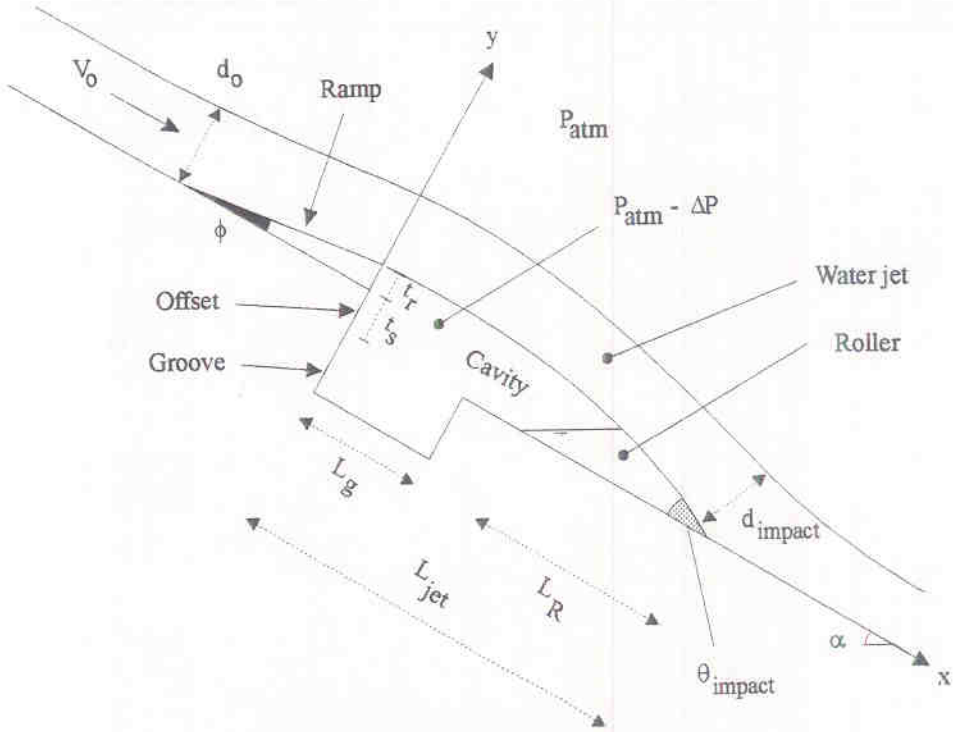

Fig. 1. Geometry of an aeration device.

named "cavity disappearance" by LAALI and MICHEL (1984), or "aerator submergence" by CHANSON (1990) and RUTSCHMANN and HAGER (1990). When the air cavity becomes filled with water, it stops playing its protecting role. At the limit the aerator becomes a large roughness and a cavitation generator (LI 1988, CHANSON 1990). For small Froude numbers, a partial or complete obstruction of the ventilation system can be caused by ice or debris blocking of the air inlets, man-made intervention or water filling of inlets. Such obstruction can reduce the local pressure ($P_{atm} - \Delta P$) in the nappe below a critical limit ($P_{atm} - \Delta P^{sub}$) and the cavity could be filled (CHANSON 1990, RUTSCHMANN and HAGER 1990).

Observations on a spillway model (CHANSON 1988) indicated that the passage from a ventilated to a filled cavity is preceded by the appearance of a large amount of spray falling from the underside of the nappe. Further as the jet curvature increases with a local pressure reduction, the upper free-surface of the flow downstream of the nappe becomes completely modified (Fig. 2). The presence of a spray along the lower air-water interface was observed by other researchers (PINTO et al. 1982, VOLKART and RUTSCHMANN 1984) for moderate to large cavity depressions, but their studies did not consider the critical case of cavity filling.

In this paper, it is shown that the onset of cavity filling can be predicted in term of a critical subpressure ΔP^{sub} for given aerator geometry and flow conditions. Then model and prototype data are examined. The analysis provides practical criterion to predict the risk of cavity filling.

2 Onset of cavity filling

2.1 *Presentation*

For low Froude numbers and large cavity subpressures, visual observations indicate that the water jet above the aerator is almost unaerated and is characterised by the presence of a roller where the

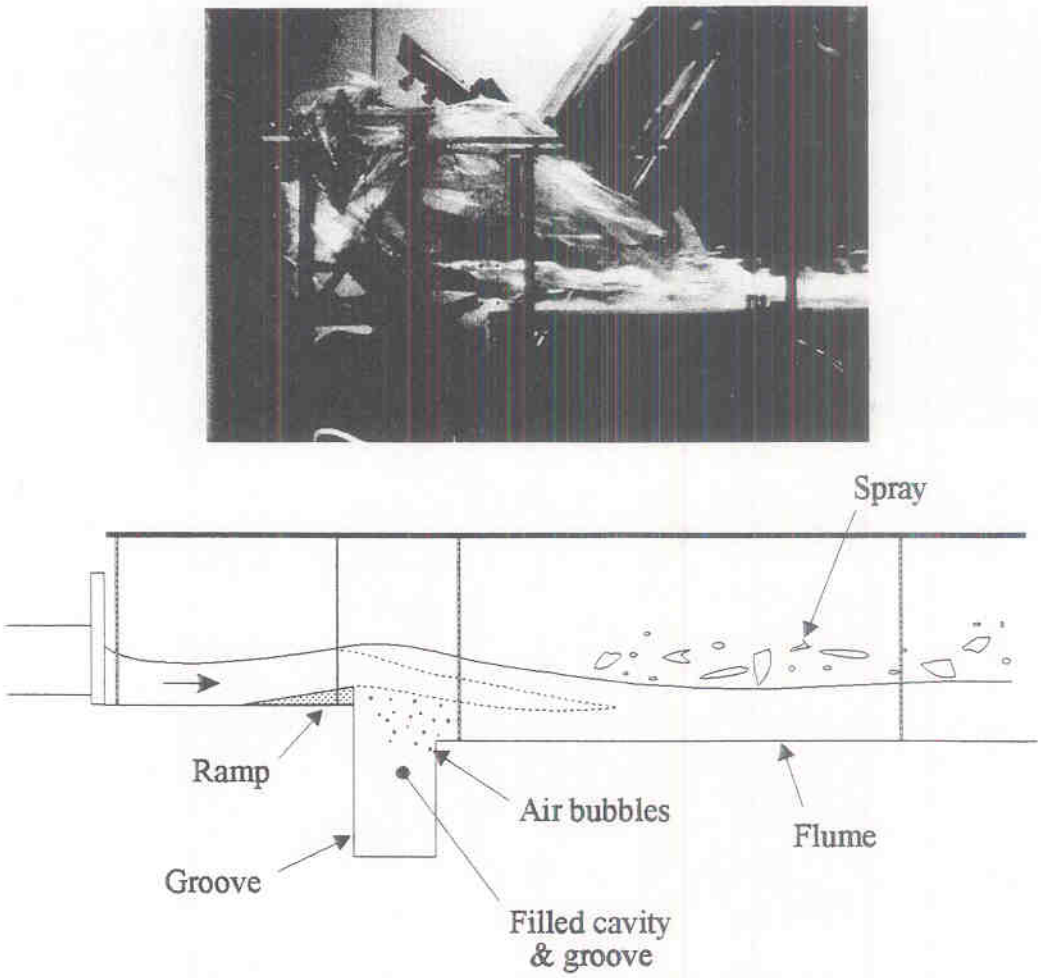

Fig. 2. Flow above the aerator of the Clyde dam spillway model during the filling of the aerator – $Fr_o = 4.0$, $d_o = 105$ mm, Geometry CH1 – Water flows from the left to the right.

water jet impacts on the spillway surface (Fig. 1). The filling of the cavity occurs when the upstream edge of the roller laps against the groove edge: i.e., if:

$$L_{jet} - L_R = L_g \tag{1}$$

where L_g is the groove length (Fig. 1). If the aeration device is grooveless, L_g must be replaced by the distance from the deflector edge to the downstream edge of the air inlets in equation (1).
The jet length L_{jet} and roller length L_R can be calculated as functions of the upstream flow conditions, the aerator geometry and the cavity subpressure (see below, eqs. (3), (4) & (10)). The critical subpressure at the onset of the cavity filling, P_N^{sub}, satisfies equation (1), where $P_N^{sub} = \Delta P^{sub}/(\rho_w g d_o)$, and cavity filling occurs for $[L_{jet} - L_R < L_g]$ or $[P_N > P_N^{sub}]$, where P_N is the pressure gradient number ($P_N = \Delta P/(\rho_w g d_o)$).

2.2 *Jet length calculations*

The jet trajectory and the cavity geometry can be computed as a function of the aerator geometry, the flow properties at the edge of the deflector and the cavity subpressure using analytical methods or numerical methods, including the finite element method.
For engineering applications, TAN (1984) developed a simple method to compute the jet length, assuming that the sub-nappe pressure acts only in the direction perpendicular to the spillway surface: i.e. the effect of the subpressure in the direction parallel to the spillway surface is ignored. At

the end of the ramp, the velocity parallel to the spillway surface is ($V_o\cos\phi$) and the velocity perpendicular to the spillway surface ($V_o\sin\phi$). Once the fluid leaves the deflector, the acceleration towards the surface is: $-g(\cos\alpha + P_N)$ and the acceleration parallel to the spillway surface is: $+g\sin\alpha$. The time t taken to reach the spillway surface is deduced from the trajectory equation:

$$t_r + t_s = (\cos\alpha + P_N)\frac{gt^2}{2} - V_o(\sin\phi)\,t \tag{2}$$

where t_s is the offset height, t_r the ramp height, V_o the velocity at the end of the deflector, and ϕ the ramp angle. The solution in term of t is:

$$t = \frac{V_o\sin\phi}{g(\cos\alpha + P_N)}\left(1 + \sqrt{1 + 2(t_r + t_s)\frac{g(\cos\alpha + P_N)}{(V_o\sin\phi)^2}}\right) \qquad \text{aerator with ramp (3a)}$$

or

$$t = \sqrt{\frac{2t_s}{g(\cos\alpha + P_N)}} \qquad \text{aerator without ramp (3b)}$$

The distance travelled during the time t is the jet length:

$$L_{jet} = \frac{g\sin\alpha}{2}t^2 + V_o(\cos\phi)\,t \tag{4}$$

where t is computed from equation (3). TAN (1984) compared his results with SCHWARTZ and NUTT's (1963) calculations and experimental values observed on the Clyde dam spillway model. The results showed no significant difference between TAN's and SCHWARTZ and NUTT's methods but all calculated values were larger than the observed jet lengths (TAN 1984).
At the impact of the water jet with the spillway bottom, the jet velocity and the jet thickness are respectively:

$$\frac{V_{impact}}{V_o} = \left(1 + 2\frac{gt}{V_o}(\cos\phi\sin\alpha - \sin\phi(\cos\alpha + P_N)) + \left(\frac{gt}{V_o}\right)^2(1 + P_N(P_N + 2\cos\alpha))\right)^{1/2} \tag{5}$$

$$\frac{d_{impact}}{d_o} = \left(1 + 2\frac{gt}{V_o}(\cos\phi\sin\alpha - \sin\phi(\cos\alpha + P_N)) + \left(\frac{gt}{V_o}\right)^2(1 + P_N(P_N + 2\cos\alpha))\right)^{-1/2} \tag{6}$$

The impact angle of the jet with the spillway bottom can be deduced from the jet trajectory equations. It yields:

$$\theta_{impact} = \tan^{-1}\left(\frac{\frac{gt}{V_o}(\cos\alpha + P_N) - \sin\phi}{\frac{gt}{V_o}\sin\alpha + \cos\phi}\right) \tag{7}$$

Note that the jet length calculations are developed neglecting the effects of the pressure from the roller. These effects are minor compared to the errors on experimental data.

2.3 *Roller calculation*

At low Froude numbers, a roller is observed when the jet reaches the spillway surface (Fig. 1). The roller is important as its weight provides the force parallel to the spillway surface which is required to prevent the flow recirculating into the cavity below the jet. At higher Froude numbers these rollers are no longer discernible but the hydrostatic pressure engendered by the pool is still necessary to change the jet from an angle to the spillway surface to parallel to this surface.
With the knowledge of the jet trajectory, the roller length can be calculated. The momentum equation resolved down the plane is:

$$-\frac{\Delta P}{2} d_{impact} \cos(\theta_{impact}) - \frac{\rho_w g}{2} (d_{impact})^2 \cos\alpha + \left(\frac{\rho_w g}{2} \frac{(L_R \sin\alpha)^2}{\sin(\alpha + \theta_{impact})} - \frac{\Delta P L_R \sin\alpha}{\sin(\alpha + \theta_{impact})} \right) \sin(\theta_{impact})$$

$$= \rho_w \frac{q_w^2}{d_{impact}} [1 - \cos(\theta_{impact})] + \rho_w g [CV] \sin\alpha \qquad (8)$$

assuming that the edges of the jet fluid have not disintegrated into spray, neglecting the shear forces on the surfaces and assuming that the magnitude of the velocity entering the control volume approximately the same as leaving it. For a large momentum inflow, it is possible to select a control volume [CV] such that the volume force is small compared to the momentum change. With this assumption, it yields:

$$\frac{1}{2} \frac{\sin(\theta_{impact})}{\sin(\alpha + \theta_{impact})} \left(\frac{L_R \sin\alpha}{d_{impact}} \right)^2 - \left(\frac{\sin(\theta_{impact})}{\sin(\alpha + \theta_{impact})} P_{N_{impact}} \right) \left(\frac{L_R \sin\alpha}{d_{impact}} \right)$$

$$- \left(\frac{1}{2} \cos\alpha (1 + P_{N_{impact}}) + (Fr_{impact})^2 [1 - \cos(\theta_{impact})] \right) = 0 \qquad (9)$$

where $Fr_{impact} = q_w / \sqrt{g d_{impact}^3}$ and $P_{N_{impact}} = \Delta P / (\rho_W g d_{impact})$. The solution of the second-degree polynomial (eq. (9)) is:

$$\left(\frac{L_R \sin\alpha}{d_{impact}} \right) = P_{N_{impact}} + P_{N_{impact}}$$

$$\times \sqrt{1 + \frac{\sin(\theta_{impact}) \{ \cos\alpha (1 + P_{N_{impact}}) + 2 (Fr_{impact})^2 [1 - \cos(\theta_{impact})] \}}{(P_{N_{impact}})^2 \sin(\alpha + \theta_{impact})}} \qquad (10)$$

For a zero pressure gradient (i.e. the same air pressure above and below the jet: $\Delta P = 0$), equation (10) yields:

$$\left(\frac{L_R \sin\alpha}{d_{impact}} \right) = \sqrt{\frac{\sin(\theta_{impact})}{\sin(\alpha + \theta_{impact})} \{ \cos\alpha + 2 (Fr_{impact})^2 [1 - \cos(\theta_{impact})] \}} \qquad (11)$$

The author (CHANSON 1988) compared successfully equation (10) with visual observations of the roller length L_R at low Froude numbers.
Note that both the jet length (eq. (3) & (4)) and the roller length (eq. (10)) are functions of the cavity subpressure ΔP. Hence equation (1) is a function the cavity subpressure.

2.4 *Discussion*

Equations (1), (4) and (10) form a system of non linear equations in terms of P_N^{sub}, L_{jet} and L_R. For a given aerator geometry (α, ϕ, t_r, t_s, L_s) and flow conditions (V_o, d_o), the cavity filling will occur if the pressure gradient number P_N is larger than P_N^{sub}.
The author measured cavity subpressures during some cavity filling events (Table 2): in one case (Fr_o = 4.02), immediately before and during the filling, and immediately before in the second case (Fr_o = 4.63). The data are compared with the calculated values of P_N^{sub} on Figure 3. Details of the aerator geometry are reported in Table 1.
TAN (1984), RUTSCHMANN (1988) and the author recorded also large cavity subpressures for flow conditions close to the occurrence of cavity filling. Their data were obtained with non-filled cavities (table 2). They are compared also with the critical subpressure for cavity filling on figure 3. During the experiments, the error on the subpressure measurement for non-filled cavities (TAN 1984, RUTSCHMANN 1988, CHANSON 1988) is about: $\delta(\Delta P)/\Delta P \sim \pm 10\%$. During filling events (CHANSON 1988), the error was about: $\delta(\Delta P)/\Delta P \sim \pm 30\%$ because of the large pressure fluctuations and the difficulties to read accurately the subpressure readings.
On Figure 3, it is interesting to note that: 1- all the subpressure data for non-filled cavity are smaller than the calculated subpressure for onset of cavity filling. And: 2- the subpressure data recorded immediately before or during cavity filling events are nearly equal or larger than the calculated P_N^{sub}. Such results, shown on Figure 3, indicate that the calculation of P_N^{sub} provides a reasonable estimate of the onset of cavity filling on spillway model. The calculation enables a reasonable prediction method of the risks of cavity filling, if the local cavity pressure can be predicted. The complete set of data and calculations are reported on Table 2.

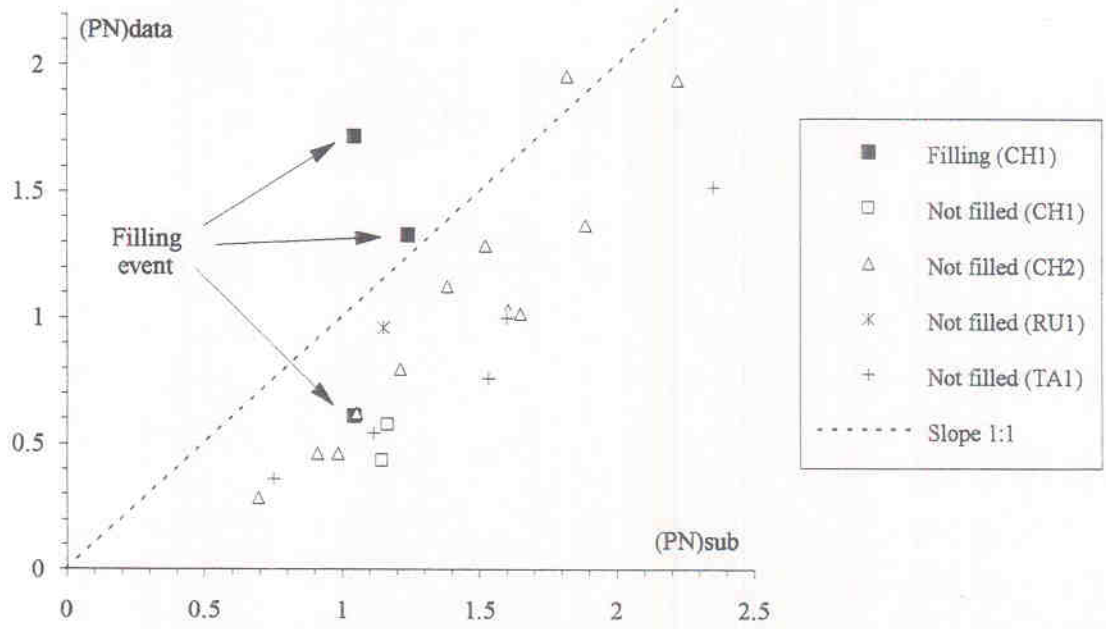

Fig. 3. Comparison between large subpressure measurements (Table 2) and the critical subpressure for onset of cavity filling P_N^{sub} (eq. (1)) – References are given in Table 1.

In practice, the cavity subpressure is a function of the duct head losses and the air entraining capacity of the flow above the aerator. The air entraining capacity of the flow is called the air demand. Although extensive investigations were performed on both model and prototype (e.g. PINTO et al. 1982, CHANSON 1990, RUTSCHMANN and HAGER 1990), there is still a lack of clear understanding of the air entrainment mechanisms. Presently, no analytical nor theoretical method exists to predict 'a priori' the air demand.

3 Experimental observations of cavity filling

3.1 *Experimental data*

Experimental observations of aerator filling were obtained by COLEMAN et al. (1983), SHI et al. (1983), TAN (1984), BRETSCHNEIDER (1986) and CHANSON (1988). The experimental flow conditions and aerator geometries of these experiments are given in table 1. The critical flow conditions for cavity filling are summarised in table 3. For the experiments of SHI et al. (1983), TAN (1984) and CHANSON (1988), the filling occurred for a complete closure of the ventilation system (i.e. $Q_{air}^{inlet} = 0$).

Table 1. Flow conditions and aerator geometry.

Aerator geometry	Ref.	Channel slope α (deg.)	Ramp angle ϕ (deg.)	Ramp height t_r (m)	Offset height t_s (m)	Groove length L_g (m)	Froude number Fr_0	Flow depth d_0 (m)	Remarks
(1)	(2)	(3)	(4)	(5)	(6)	(7)	(8)	(9)	(10)
Aerator with ramp									
SH1	(I)	0	5.7	0.01	0.0	(--)	2.9 to 21.9	0.06 to 0.18	Fengjiashan spillway model. W = 0.2 m.
SH2	(I)	10	5.7	0.01	0.0	(--)	2.9 to 21.9	0.06 to 0.18	
SH3	(I)	30	5.7	0.01	0.0	(--)	2.9 to 21.9	0.06 to 0.18	
SH4	(I)	49	5.7	0.01	0.0	(--)	2.9 to 21.9	0.06 to 0.18	
CO1	(II)	7.125	1.9	0.005	0	(--)	(--)	(--)	Uribante spillway model
RU1	(IV)	34.5	4	0.0095	0	0.2	8.7	0.10	Configuration 1E.
CH1	(V)	52.3	5.7	0.03	0.03	0.19	3.4 to 23.4	0.023to 0.11	Clyde dam spillway model. W = 0.25 m.
Aerator with offset									
TA1	(III)	51.3	0	0.0	0.03	0.19	5.0 to 15.4	0.05 to 0.11	Clyde dam spillway model. W = 0.25 m
CH2	(V)	52.3	0	0	0.03	0.19	5.4 to 23.6	0.023 to 0.083	
Horizontal groove									
BR1	(IV)	0	0	0	0	0.02 to 0.10	(--)	0.004 to 1	Flow above a groove only

(I): Shi et al. (1983)
(II): Coleman et al. (1983)
(III): Tan (1984)
(IV): Bretschneider (1986)
(V): Chanson (1988)
(VI): Rutschmann (1988)
(--): Unavailable information

For aerator geometries with a ramp, the experiments of SHI et al. (1983), COLEMAN et al. (1983) and CHANSON (1988) suggest that cavity filling occurs for Froude numbers less than a critical value:

$$Fr_o < Fr^{sub} = f_1\left(\phi; \frac{t_r}{d_0}; \alpha; \frac{t_s}{d_0}\right) \tag{12}$$

where Fr^{sub} is the critical Froude number at which filling occurs. Figure 4 shows: 1) the critical conditions of filling Fr^{sub} at which cavity filling starts, obtained by SHI et al. (1983) and CHANSON (1988), and 2) two experimental observations of filled cavities reported by COLEMAN et al. (1983) (i.e. $Fr_o < Fr^{sub}$).

For aerators with an offset and no ramp (i.e. $t_r = 0$, $\phi = 0$), the experiments of TAN (1984) and CHANSON (1988) indicate that filling occurs for flow depths larger than a critical value: i.e. if

$$\frac{t_s}{d_0} < \frac{t_s}{(d_0)^{sub}} = f_2(\alpha) \tag{13}$$

where $(d_o)^{sub}$ is a characteristic depth above which filling occurs. For a channel slope of about 52 degrees, the data of TAN (1984) and CHANSON (1988) indicate that: $t_s/(d_o)^{sub} = 0.61$. Their experiments were performed in the same channel but with different approach flow conditions (CHANSON 1990). The upstream flow conditions were more turbulent for TAN's experiments. The identical results obtained by TAN (1984) and CHANSON (1988) show a good consistency in the data and reproductibility of the submergence process for that particular slope.

Table 2. Experimental data of extreme cavity subpressures.

Aerator geometry	d_o (m)	Fr_o	$\frac{Q_{air}^{inlet}}{Q_w}$	P_N	P_N^{sub} [a]	Comments
(1)	(2)	(3)	(4)	(5)	(6)	(7)
Cavity filling						
CH1	0.105	4.02	0.0	0.611[b]	1.044	Before filling.
		4.02	0.0	1.728 [c]	1.044	During filling.
	0.107	4.63	0.0	1.33 [b]	1.240	Before filling.
Cavity not filled						
CH1	0.060	4.63	~ 0	0.307	1.195	Cavity not
	0.077	4.39	~ 0	1.145	1.145	filled. [d]
	0.77	4.44	~ 0	1.165	1.165	
CH2	0.051	10.72	0.033	1.032	1.605	Cavity not
	0.051	11.01	0.039	1.017	1.650	filled.
	0.051	12.43	0.044	1.369	1.888	
	0.051	14.56	0.041	1.941	2.220	
	0.067	5.60	0.029	0.286	0.695	
	0.067	6.73	0.023	0.461	0.911	
	0.067	7.53	0.024	0.621	1.052	
	0.067	8.44	0.028	0.796	1.212	
	0.067	10.36	0.037	1.287	1.522	
	0.067	12.32	0.035	1.955	1.821	
	0.082	7.15	0.027	0.463	0.985	
	0.082	9.64	0.031	1.125	1.383	
TA1	0.05	10.3	0.0	1.52	2.35	Cavity not
	0.05	10.7	0.0	1.0	1.6	filled.
	0.05	15.4	0.07	0.760	1.534	
	0.10	5.80	0.037	0.360	0.752	
	0.10	8.05	0.032	0.540	1.115	
RU1	0.10	8.71	0.058	0.960	1.152	Cavity not filled.

(a): computed using equations (1), (4) and (10), (b): recorded immediatly before cavity filling,
(c): recorded during the filling of the cavity for the same run as (b), (d): air inlets not perfectly sealed

For ventilated cavities behind an offset in horizontal channels, LAALI and MICHEL (1984) reported cavity filling when the air inlets are fully-closed (i.e. $Q_{air}^{inlet} = 0$. No quantitative measurements near cavity disappearance were reported).

3.2 *Discussion*

The filling of an aerator cavity can occur by an increase of the flow depth or a decrease of the Froude number. As a result, the filling of the cavity may occur for discharges lower than the design

discharges as observed by COLEMAN et al. (1983). The data of COLEMAN et al. (1983) (for filled cavities) indicate Froude numbers that are larger than the other model data. Experimental investigations performed with a wide range of channel slopes and aerator configurations (e.g. LOW 1986, RUTSCHMANN 1988) showed that the cavity subpressure number P_N for small or zero air discharges increases with decreasing ramp angle ϕ, for identical flow conditions. As a result, cavity filling of aerators with flat ramps (e.g. COLEMAN et al. 1983) is expected to occur at larger Froude numbers than for aerators with a large ramp angle (e.g. SHI et al. 1983, CHANSON 1988).

Table 3. Conditions for cavety filling.

Ref. (1)	Aerator geometry (2)	Condition for filling (3)	Remarks (4)
Aerator with ramp			
SHI et al. (1983)	SH1, SH2, SH3, SH4	$\frac{t_r}{(R_H)_o} < 23.5 \left(\frac{\cos\alpha \cos\phi}{\frac{V_o}{\sqrt{g\,(R_H)_o}}} \right)^3$	For a wide channel it yields : $Fr_o < 2.86 \cos\alpha \cos\phi \sqrt[3]{d_o/t_r}$
CHANSON (1988)	CH1	$Fr_o < 2.77 + 0.94 \frac{d_o}{t_s}$	
Aerator without ramp			
TAN (1984)	TA1	$\frac{t_s}{d_o} < 0.6$	Experiments performed in 1983.
CHANSON (1988)	CH1	$\frac{t_s}{d_o} < 0.62$	Experiments performed in 1986-87.
Horizontal groove			
BRETSCHNEIDER (1986)	BR1	$Fr_o < 5.8$	
Cavity behind blunt body			
ROBERTSON (1965)	Very blunt bodies (normal discs and plates)	$\sigma < 0.5$	Note : $\sigma \sim 2 \frac{\cos\alpha + P_{atm}/(\rho_w g d_o)}{Fr_o^2}$

Notes : $(R_h)_0$: hydraulic radius in the approach flow conditions

For aerator geometries with a ramp and no offset (i.e. $t_s = 0$), operating conditions of existing prototype aerators (Table 4) are presented also on Figure 4. The flow conditions for the spillways of Amaluza, Colbun, Emborcacao, Fengman, Foz de Areia and Tarbela are operating flow conditions for which no cavity filling is observed. Figure 4 would suggest some discrepancies between the observations on spillway models (Tables 1 and 3) and the operating conditions of prototypes. On prototypes, the air supply system of the aerator was either fully open or half-open while the data of SHI et al. (1983) and CHANSON (1988) were obtained with fully closed air ducts. Therefore these model results are more pessimistic than prototype conditions.

Table 4. Geometry of prototype spillway aerators.

Spillway (1)	Channel slope α (deg.) (2)	Ramp angle ϕ (deg.) (3)	Ramp height t_r (m) (4)	Offset height t_s (m) (5)	Reference (6)
Amaluza, Ecuador	67.5	5.7	0.06	0	RUTSCHMANN (1988)
Colbun, Chile	27.1	9.8	0.22	0	ALVARDO et al. (1988)
Emborcacao, Brazil	10.2	7.12	0.30 0.20	0	RUTSCHMANN (1988)
Fengman, China	52.0	1.15	0.2	0	ZHOU and WANG (1988)
Foz de Areia, Brazil	14.5	7.12	0.19 0.14 0.10	0	PINTO et al. (1982)
Tarbela, Pakistan	0	7.12	0.14	0	PINTO (1989)

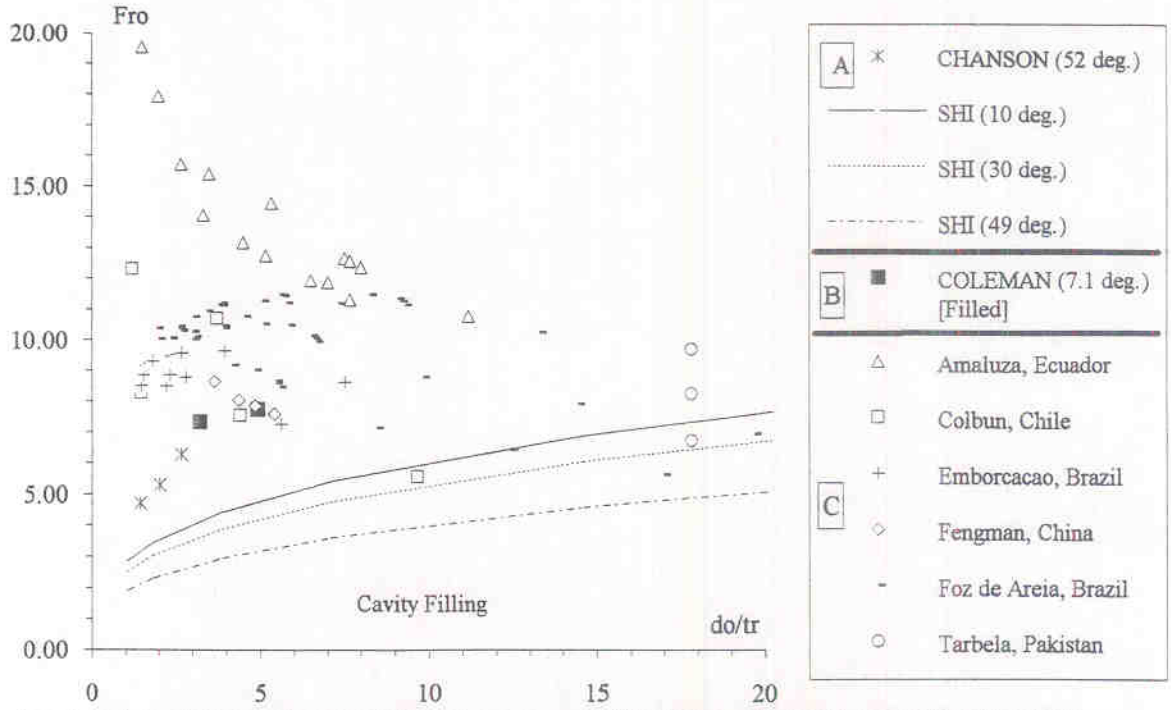

A: critical conditions of cavity filling (i.e. $Fr_o = Fr^{sub}$): SHI et al.(1983), CHANSON (1988)
B: operating condition with filling (i.e. $Fr_o = Fr^{sub}$): COLEMAN et al. (1983)
C: operating conditions on prototype without filling (i.e. $Fr_o > Fr^{sub}$): AMULAZA, COLBUN, EMBORCACOA, FENGMAN, FOZ DE AREIA, TARBELA

Fig. 4. Conditions of filled cavities for aerators with ramp.

In term of model-prototype agreement, the present investigation suggests that the mechanism of cavity filling depends upon the cavity subpressure and its effect on the jet and roller calculations, but not upon the air entrainment processes. For scaling purpose, the relevant dimensionless parameter is the pressure gradient number P_N. P_N is proportional to the average pressure gradient in the direction normal to the streamlines. With spillways located in high mountains, the effect of the atmospheric pressure must be taken also into account. Indeed, for atmospheric pressures ranging from 1×10^4 Pa to 2×10^4 Pa, LAALI and MICHEL (1984) showed that, for a given pressure gradient number P_N and Froude number Fr, the air inlet discharge decreases when the ambient pressure above the jet P_o decreases. Their results suggest that the performances of aerator located at high altitude may be affected by the lower atmospheric pressure.

In the previous section, we have shown that equation (1) would enable a reasonable prediction of cavity filling if the cavity subpressure could be predicted as a function of the aerator geometry and flow conditions. In practice, the cavity subpressure cannot be predicted theoretically. The information summarised on Figure 4 can be considered as a conservative set of guidelines for aerators with ramps; it indicates that flow conditions with Froude numbers less than 7 to 8 should be investigated with a physical model to verify the risks of cavity filling.

4 Conclusion

For low flow rates and partial or complete obstruction of the air supply system, the air cavity above an aerator can fill and the aeration device stops preventing cavitation damage. Further, a filled-cavity deflector might act as a cavitation generator, even at low Froude numbers.

Cavity filling occurs when the cavity subpressure exceeds a critical value (eq. (1)). The critical pressure number P_N^{sub} for the onset of cavity filling can be calculated from the aerator geometry

and the flow conditions (eqs. (1), (4) and (10)). Comparison with experimental observations suggests that these calculations provide a reasonable prediction of cavity filling.

In practice, for the design of new aerators, it is not presently possible to predict the cavity subpressure without model experiments. In such cases, the experience of cavity filling presented in this paper, for ten aerator geometries, may provide information to avoid the filling. For an aerator with a ramp, the cavity filling occurs when the Froude number becomes less than a critical value of about 7 to 8 (Fig. 4). For an aerator with an offset and without a ramp, the filling of the cavity occurs above a critical value of the flow depth.

Most experimental observations of cavity filling were obtained on spillway models. Further experimental data on prototypes are required to check possible scale effects.

5 Acknowledgement

The author wishes to acknowledge the helpful comments of Mr CHEN Ming-Jen, Hydraulic Research Laboratory, National Taiwan University.

List of symbols

d	1. flow depth (m) measured perpendicular to the channel bottom; 2. water jet thickness (m) measured perpendicular to the jet streamlines;
d_{impact}	water jet thickness (m) at the jet impact, measured perpendicular to the jet streamlines (Fig. 1);
d_o	depth of flow at the end of the approach flow region (m);
Fr	Froude number defined as: $Fr = q_w \sqrt{g d^3}$;
g	gravity constant (m/s^2);
L_g	groove length (m);
L_{jet}	jet length (m);
L_R	roller length (m);
P_{atm}	atmospheric pressure (Pa): i.e. pressure above the flow;
P_N	pressure gradient number defined as: $P_N = \Delta P/(\rho_W g d))$
Q_{air}^{inlet}	air discharge (m^3/s) supplied by the air ducts;
Q_w	water discharge (m^3/s);
q_w	water discharge per unit width (m^2/s);
$(R_H)_o$	hydraulic radius (m) at the end of the approach flow region;
t	time (s);
t_r	ramp height (m);
t_s	offset height (m);
V	velocity (m/s);
V_o	velocity (m/s) at the end of the approach flow region;
W	channel width (m);
α	spillway slope;
ΔP	difference between the pressure above the flow and the air pressure in the cavity
ϕ	ramp angle;
θ	angle of the water jet with the channel bottom;
ρ_W	water density (kg/m^3);
σ	cavitation index (also called Thoma number);

Subscript

impact flow conditions at the end of the water jet, near the impact of the jet with the spillway bottom;

o initial flow conditions;

Superscript

sub onset of cavity filling.

Bibliography

ALVARDO, L., MERY, A., and PINTO, N.L. de S. (1988). "Design and Operation of the Colbun Spillway and Low-Level Outlet." Intl Water Power and Dam Construction, 40 (4), pp. 38–42.

BRETSCHNEIDER, H. (1986). "Der Begin des Lufteintrages bei Sohlennischen." ("The Beginning of Air Entrainment at Bottom Grooves.") Die Wasserwirtschaft, Vol. 76, No. 5, pp. 203–207 (in German).

CHANSON, H. (1988). "Study of Air Entrainment and Aeration Devices on Spillway Model." Research Report No. 88-8, Univ. of Canterbury, New Zealand.

CHANSON, H. (1990). "Study of Air Demand on Spillway Aerator." Jl of Fluids Engrg., ASME, Vol. 112, Sept., pp. 343–350.

COLEMAN, H.W., SIMPSON, A.R., and DE GARCIA, L.M. (1983). "Aeration for Cavitation Protection of Uribante Spillway." Proc. of the Conf. on Frontiers in Hydraulic Engineering, ASCE-MIT, Cambridge, USA, H.T. SHEN Editor, pp. 438–443.

FALVEY, H.T. (1982). "Predicting Cavitation in Tunnel Spillways." Intl Water Power and Dam Construction, Aug. 1982, pp. 13–15.

LAALI, A.R., and MICHEL, J.M. (1984). "Air Entrainment in Ventilated Cavities: Case of the Fully Developed 'Half- Cavity'." Jl of Fluids Eng., Trans. ASME, Sept., Vol. 106, p.319.

LI, SHUFANG (1988). "Design and Experience of Aerations Steps on the Left Bank Spillway of the Lubuge Hydroelectric Power Project. " Proc. of the Intl Symp. on Hydraulics for High Dams, IAHR, Beijing, China, pp. 688-695.

LOW, H.S. (1986). "Model Studies of Clyde Dam Spillway aerators." Research Report No. 86-6, Dept. of Civil Eng., Univ. of Canterbury, Christchurch, New Zealand.

PINTO, N.L. de S. (1989). "Designing Aerators for High Velocity Flow." Intl Water Power and Dam Construction, 7, pp. 44–48.

PINTO, N.L. DE S., NEIDERT, S.H., and OTA, J.J. (1982). "Aeration at High Velocity Flows." Water Power and Dam Construction, No. 34 (2) pp. 34-38, No. 34 (3) pp. 42-44.

ROBERTSON, J.M. (1965). "Hydrodynamics in Theory and Application." Prentice-Hall International, London, UK, 1965.

RUTSCHMANN, P. (1988). "Belüftungseinbauten in Schussrinnen - Wirkungsweise, Formgebung und Berechnung von Schussrinnenbelüftern." Ph.D. Dissertation ETH No. 8514, Eidgenössische Technische Hochschule Zürich, Zürich, Switzerland. (in German)

RUTSCHMANN, P., and HAGER, W.H. (1990). "Air Entrainment by Spillway Aerators." Jl of Hyd. Engrg., ASCE, Vol. 116, No. 6, pp. 765–762.

SCHWARTZ, H.I., and NUTT, L.P. (1963). "Projected Nappes Subject to Transverse Pressure." Jl of Hyd. Div., Proc. ASCE, July, pp. 97–104.

SHI, Q., PAN, S., SHAO, Y., and YUAN, X. (1983). "Experimental Investigation of Flow Aeration to prevent Cavitation Erosion by a Deflector." Shuili Xuebao (Jl of Hydraulic Engrg.), Beijing, China, Vol. 3, pp. 1–13 (in Chinese).

TAN, T.P. (1984). "Model Studies of Aerators on Spillways." Research Report Ref. 84-6, Univ. of Canterbury, New Zealand.

VOLKART, P., and RUTSCHMANN, P. (1984). "Rapid Flow in Spillway Chutes with and without Deflectors – A Model-Prototype Comparison." Proc. of the Intl. Symp. on Scale Effects in Modelling Hydraulic Structures, IAHR, Esslingen, Germany, H. KOBUS editor, paper 4.5.

ZHOU, LINTAI, and WANG, Junjie (1988). "Erosion Damage at Fengman Spillway Dam and Investigation on Measures of preventing Cavitation." Intl Symp. on Hydraulics for High Dams, IAHR, Beijing, China, pp. 703–709.